CIRP Annals - Manufacturing Technology 63 (2014) 125–128

Contents lists available at ScienceDirect

CIRP Annals - Manufacturing Technology

journal homepage: http://ees.elsevier.com/cirp/default.asp

The effects of tool edge radius on drill deflection and hole misalignment in deep hole gundrilling of Inconel-718

K.S. Woon [a], A. Chaudhari [b], M. Rahman (1)[b,*], S. Wan [c], A. Senthil Kumar [b]

[a] Singapore Institute of Manufacturing Technology, 71, Nanyang Drive, 638075 Singapore, Singapore
[b] National University of Singapore, 10, Kent Ridge Crescent, 119260 Singapore, Singapore
[c] Institute of High Performance Computing, 1, Fusionopolis Way, #16-16 Connexis, 138632 Singapore, Singapore

ARTICLE INFO

Keywords:
Deep hole drilling
Cutting edge
Hole straightness

ABSTRACT

Straightness control in gundrilling of deep, thin-walled holes on Inconel-718 is challenging due to insufficiently explored phenomena governed by the tool edge radius effects. Such effects are activated by conservative drilling conditions for Inconel-718, which transforms the chip formation mode to a thrust-dominated mechanism. Critical changes in force generation are thus resulted, which affect the characteristics of drill deflection and thin wall deformation. In consequence, the drill's self-piloting capability deteriorates – leading to uncontrollable deflection and hole misalignment. A mechanistic model uniting the underlying force, drill deflection, wall deformation and process kinematics is proposed and substantiated, as well.

1. Introduction

Market demand for deep holes with thin walls on Inconel-718 is growing rapidly in the oil and gas sector for the manufacturing of advanced downhole equipment. The deep holes serve as conduits for power supply, data communication, air-circuit logic flow, remote monitoring and control with sensors and electronics embedded to special Inconel-718 drill collars for deepwater oil exploration. To construct such deep holes, gundrilling is a natural choice with its vast successful applications on conventional materials like Al alloys, cast irons and alloyed steels. But the same drilling technology has not been gaining ground with this Inconel-718 application due to stringent requirements as follows: (i) extreme length-to-diameter ratios of up to 625; (ii) adjacent thin walls as fine as 5 mm; (iii) minimum yield strength of 1000 MPa.

Rapid degradation of the carbide gun drill tips is one of the most serious production issues, largely driven by continuous work hardening. An ever increase in cutting force and heat generation is thus resulted throughout the process. Coupled with the strong heat resistivity properties of Inconel-718 relative to its extremely low conductivity, gun drills degrade rapidly and fail under harsh thermal and mechanical loading conditions, despite the use of specially formulated drilling oil or coolant at high pressure.

To prevent catastrophic drill failures, industry practitioners often approach such applications with conservative parameters. According to [1–3], feed rates f for drilling Inconel-718 are suppressed between 8.95 and 23.3 mm/min. Combining with low rotational speeds ω between 873 and 1650 rpm to minimize work hardening, uncut chip thickness t_0 is reduced to micron scale between 8.9 and 14.1 μm. Commercial gun drills for drilling Inconel-718 are found to have cutting edge sharpness, defined as tool edge radius r_e that range between 4.84 and 6.14 μm (based on 60 drills from 4 brands). A sample measurement is shown in Fig. 1. Thus, along with the downscaling of cutting magnitude that approaches r_e in micron scale, the tool edge radius effects on the process mechanics are activated.

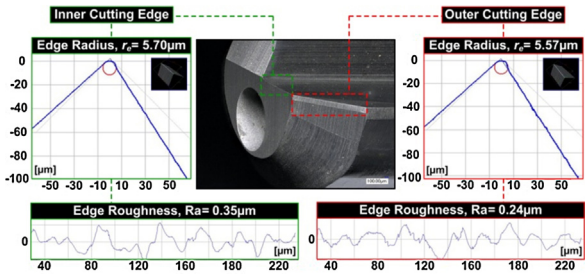

Fig. 1. Cutting edge measurement of a gun drill with Alicona Infinite Focus microscope according to ISO 25178-6, based on non-contact areal based method with focus variation.

Under the governance of tool edge radius effects, chip formation is shifted from a cutting-dominated mechanism to a thrust-dominated mechanism, with the promotion of material ploughing. Along with this, the resultant force vector on the cutting edges is diverted from the cutting direction, which forces the drill against the hole and resulted in severe frictional heating and normal supporting force on the bearing pads. As a consequence, the adjacent thin walls are thermally softened and mechanically deformed. By then, the drill is susceptible to buckling due to the change in axial thrust force and deflects uncontrollably towards

* Corresponding author.

http://dx.doi.org/10.1016/j.cirp.2014.03.075
0007-8506/© 2014 CIRP.

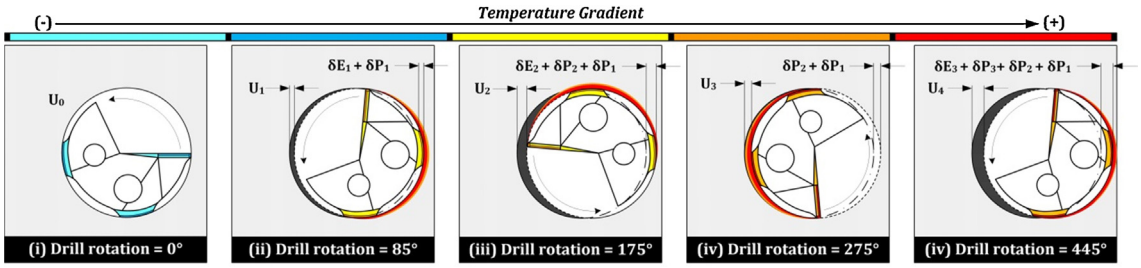

Fig. 2. Hole misalignment and drill deflection, where U_i is drill deviation; E_i is elastic deformation; P_i is plastic deformation. (i) $U_0 = 0$ before cutting commences; (ii) $U_1 = \delta E_1 + \delta P_1$ after primary deformation; (iii) $U_2 = \delta E_2 + \delta P_2 + \delta P_1$ after primary elastic recovery and secondary deformation; (iv) $U_3 = \delta P_2 + \delta P_1$ after secondary elastic recovery; (v) $U_4 = \delta E_3 + \delta P_2 + \delta P_2 + \delta P_1$ after tertiary deformation and elastic recovery. *Remark*: Temperature increase of the drill and deformation zone due to frictional heating are illustrated with a simplified colour scheme.

the softer thin walls. Eventually, severe hole misalignment is produced through cyclic repetition of such mechanism throughout the process, as conceptually illustrated in Fig. 2.

In spite of the significance of tool edge radius effects, little is known of its actual impact on gundrilling. Most investigations in the past were focused on drilling conventional materials that do not observe similar phenomena. This forms the basis of this study to develop quantitative understanding of the tool edge radius effects on hole misalignment through analytical modelling of force generation, drill deflection, wall deformation and process kinematics. A mechanistic model that accounts for these effects is proposed and substantiated with two sets of experiments.

2. Model development

A mechanistic modelling approach was adopted. Cutting forces of the process are first derived. Then the effects of the forces on drill deflection and wall deformation are established. Lastly, a unified model is proposed to describe the kinematics.

2.1. Cutting force

With the significance of tool edge radius effects, the new model has to account for cutting and ploughing. As shown in Fig. 3, the inner *i* and outer *o* cutting edges of the gun drill are divided into a finite number of cutting elements with a width:

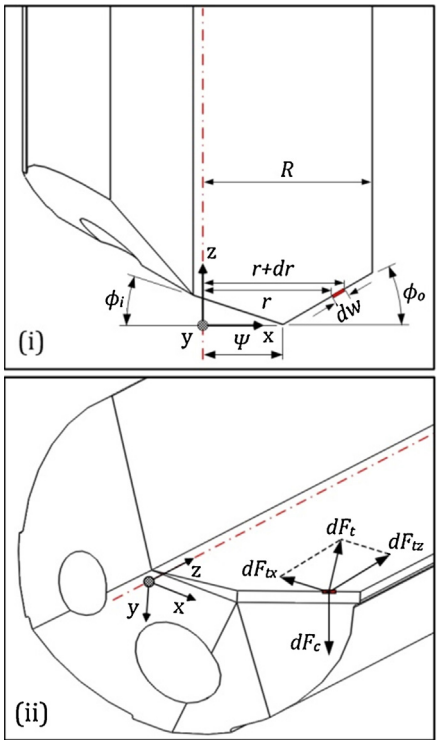

Fig. 3. Modelling of force generation on the inner and outer cutting edges of a gun drill. (i) Top view; and (ii) isometric view.

$$dw_{i,o} = \frac{dr}{\cos\phi_{i,o}} \tag{1}$$

where r is the drill radius while ϕ_i and ϕ_o are the inner and outer cutting angles. Uncut chip thickness on the cutting edges is:

$$t_0 = f\cos\phi_{i,o} \tag{2}$$

Instantaneous shear force over the cutting element is defined as:

$$dF_s = \frac{kt_0 dw}{\sin\phi_n} = \frac{k\,f dr}{\sin\phi_n} \tag{3}$$

where k is material shear flow stress and ϕ_n is the instantaneous shear angle determined from the Johnson-Cook model with the underlying parameters reported by Klocke et al. [4], as identified with an inverse methodology.

Thus, the instantaneous cutting and thrust components are:

$$dF'_c = dF_s\frac{\cos(\phi_n - \gamma_n)}{\cos\chi_n} \quad \text{and} \quad dF'_t = dF_s\frac{\sin(\phi_n - \gamma_n)}{\cos\chi_n} \tag{4}$$

where χ_n is the angle between dF_s and resultant of dF'_c and dF'_t.

Effective rake angle Y_n is governed by t_0 and r_e [5], in which:

$$\gamma_n = \sin^{-1}\left(\frac{t_0}{r_e} - 1\right) \quad \text{when} \quad \frac{t_0}{r_e} < \left(\frac{t_0}{r_e}\right)_{\lim}; \quad \text{or} \quad \gamma_n = \gamma \quad \text{when} \quad \frac{t_0}{r_e} > \left(\frac{t_0}{r_e}\right)_{\lim} \tag{5}$$

$$\text{where} \quad \left(\frac{t_0}{r_e}\right)_{\lim} = 1 + \sin\gamma \tag{6}$$

Ploughing components [6] in the directions of dF'_c and dF'_t are:

$$dF''_c = \sigma dw_{i,o} r_e \tan\left(\frac{\pi}{4} + \frac{\gamma_n}{2}\right) \quad \text{and} \quad dF''_t = \sigma dw_{i,o}\left(1 + \frac{\pi}{2}\right) r_e \tan\left(\frac{\pi}{4} + \frac{\gamma_n}{2}\right) \tag{7}$$

Total cutting and thrust forces on inner and outer edges are:

$$F_{ci} = \int_0^{\psi}(dF'_{ci} + dF''_{ci}) \quad \text{and} \quad F_{ti} = \int_0^{\psi}(dF'_{ti} + dF''_{ti}) \tag{8}$$

$$F_{co} = \int_{\psi}^{R}(dF'_{co} + dF''_{co}) \quad \text{and} \quad F_{to} = \int_{\psi}^{R}(dF'_{to} + dF''_{to}) \tag{9}$$

Transforming the localized forces to the main axes, they become:

$$F_x = F_{ti} \times \sin\phi_i - F_{to} \times \cos\phi_0 \tag{10}$$

$$F_y = F_{ci} + F_{co} \tag{11}$$

$$F_z = F_{ti} \times \cos\phi_i + F_{to} \times \cos\phi_0 \tag{12}$$

2.2. Drill deflection

Drill deflection is primarily caused by F_z where the long and slender structure is compressed and buckled. A modified version with Euler's beam theory is hereby proposed. As shown in Fig. 4,